Defective uptake of triglyceride-associated fatty acids in adipose tissue causes the SREBP-1c-mediated induction of lipogenesis

Elke M. Wagner,[1,*] Dagmar Kratky,[1,†] Guenter Haemmerle,[*] Andelko Hrzenjak,[†] Gert M. Kostner,[†] Ernst Steyrer,[†] and Rudolf Zechner[2,*]

Institute of Molecular Biology, Biochemistry, and Microbiology,* and Institute of Medical Biochemistry and Medical Molecular Biology,† University of Graz, Graz, Austria

Abstract **Lipoprotein lipase (LPL) is the only known enzyme in the capillary endothelium of peripheral tissues that hydrolizes plasma triglycerides and provides fatty acids (FAs) for their subsequent tissue uptake. Previously, we demonstrated that mice that express LPL exclusively in muscle develop essentially normal fat mass despite the absence of LPL and the deprivation of nutritionally derived FAs in adipose tissue (AT). Using this mouse model, we now investigated the metabolic response to LPL deficiency in AT that enables maintenance of normal AT mass. We show that the rate of FA production was 1.8-fold higher in LPL-deficient AT than in control AT. The levels of mRNA and enzymatic activities of important enzymes involved in FA and triglyceride biosynthesis were induced concomitantly. Increased plasma glucose clearing and ^{14}C-deoxyglucose uptake into LPL-deficient mouse fat pads indicated that glucose provided the carbon source for lipid synthesis. Leptin expression was decreased in LPL-deficient AT. Finally, the induction of de novo FA synthesis in LPL-deficient AT was associated with increased expression and processing of sterol regulatory element binding protein 1 (SREBP-1), together with an increase in INSIG-1 expression. These results suggest that in the absence of LPL in AT, lipogenesis is activated through increased SREBP-1 expression and processing triggered by decreased availability of nutrition-derived FAs, elevated insulin, and low leptin levels.**—Wagner, E. M., D. Kratky, G. Haemmerle, A. Hrzenjak, G. M. Kostner, E. Steyrer, and R. Zechner. **Defective uptake of triglyceride-associated fatty acids in adipose tissue causes the SREBP-1c-mediated induction of lipogenesis. *J. Lipid Res.* 2004.** 45: **356–365.**

Supplementary key words fatty acid biosynthesis • lipoprotein lipase • lipogenic enzymes • sterol regulatory element binding protein • insulin-induced gene • leptin • polyunsaturated fatty acid

Adipose tissue (AT) is crucially involved in the storage of food calories during periods of infrequent nutrient uptake and in the regulated release of fatty acids (FAs) as energy substrate during periods of starvation. The opposing processes of FA storage and FA mobilization in and from fat depots are catalyzed by lipases. Lipoprotein lipase (LPL) is expressed in many nonhepatic tissues, with the highest expression levels found in AT and muscle. The enzyme is positioned at the lumenal surface of the capillary endothelium and hydrolyzes lipoprotein-associated triglycerides (TGs), and the resulting FAs are absorbed by the underlying tissue (1, 2). Conversely, hormone-sensitive lipase (HSL), and possibly other yet unidentified lipases, facilitate the hormonally controlled hydrolysis of intracellular TG stores in AT for the subsequent release of FA into the vascular system (3, 4).

Recently, a mouse model was established that expressed LPL exclusively in muscle but lacked LPL in AT. These animals were bred from transgenic mice that overexpressed a human LPL minigene under the muscle-specific control of the mouse creatine kinase promoter (MCK mice) and heterozygous LPL knockout mice (5, 6). Animals that expressed the LPL transgene only in muscle but lacked both endogenous mouse LPL alleles (L0-MCK mice) gained normal body weight and AT mass despite the complete absence of LPL in AT (5). However, the FA composition of TG in LPL-deficient AT differed markedly from control fat, exhibiting an 88% decrease of linoleic acid and linolenic acid and a concomitant 38 and 248% increase of palmitic and palmitoleic acid, respectively (5). The observed

Manuscript received 1 July 2003 and in revised form 30 September 2003.

Published, JLR Papers in Press, November 1, 2003.
DOI 10.1194/jlr.M300293-JLR200

Abbreviations: ACC, acetyl-CoA carboxylase; AT, adipose tissue; ATP-CL, ATP-dependent citrate lyase; DGAT, acyl-CoA:diacylglycerol acyltransferase; FA, fatty acid; FAS, fatty acid synthase; G6PDH, glucose-6-phosphate dehydrogenase; HSL, hormone-sensitive lipase; INSIG, insulin-induced gene; LPL, lipoprotein lipase; MCK, mouse creatine kinase; ME, malic enzyme; PDH, pyruvate dehydrogenase; PPAR, peroxisome proliferator-activated receptor; SCD, stearoyl-CoA desaturase; SREBP, sterol regulatory element binding protein; TG, triglyceride.

[1] E. M. Wagner and D. Kratky contributed equally to this work.

[2] To whom correspondence should be addressed.
e-mail: rudolf.zechner@uni-graz.at

decrease in polyunsaturated and, therefore, essential FA suggested that the cellular import of nutrient-derived FA was drastically reduced in L0-MCK mice, supporting the concept that LPL represents the rate-limiting enzyme for the uptake of lipoprotein-associated FAs (7, 8). We have further speculated that in the absence of AT-LPL, the maintenance of normal fat mass must have been achieved by the de novo synthesis of FAs and lipid from alternative substrates such as glucose (5).

In this study, we show that the absence of LPL in AT results in increased glucose uptake in adipocytes and in the induction of the endogenous synthesis of FAs and TG. We propose that in LPL-deficient AT, the decreased uptake of dietary FAs, increased plasma insulin levels, and decreased plasma leptin concentrations cause the induction of sterol regulatory element binding protein-1 (SREBP-1) expression and processing, which in turn activates the lipogenic program to maintain normal fat mass.

EXPERIMENTAL PROCEDURES

Animals

L0-MCK mice express a human LPL minigene under the control of the MCK promoter in the absence of endogenous mouse LPL (5, 6). L0-MCK mice were generated as described previously (5, 6). Nontransgenic littermates expressing two intact endogenous mouse LPL alleles in AT (L2) were used as controls. Genotypes were identified from tail tip DNA by PCR analysis as reported (5). All animals were maintained on a regular light-dark cycle (14 h of light, 10 h of dark) and kept on a standard laboratory chow diet containing 4.5% fat and 21% protein (SSNIFF, Germany) with free access to water. Male transgenic and control mice aged 3–6 months were investigated concomitantly at each set of experiments.

Plasma parameters

Blood was collected from overnight fasted, fed, or fasted/2 h refed animals by retro-orbital bleeding, and EDTA-plasma was prepared within 20 min. Blood glucose was measured immediately after the plasma preparation using a commercial kit (Merck, Darmstadt, Germany). Free FAs were measured enzymatically (Wako Chemicals, Neuss, Germany). Insulin, glucagon, and leptin plasma protein concentrations from overnight fasted and 2 h refed mouse sera were measured by radioimmunoassays (Linco, MO). All assays were performed according to the manufacturer's protocols.

De novo FA and TG biosynthesis rate

The rate of endogenous FA production was determined in male L0-MCK and L2 mice using ^3H_2O as a tracer (9). Mice were fed 3 h per day for a period of 3 weeks. On the day of the experiment, 1 mCi of ^3H_2O was injected into the tail vein after 2 h of refeeding, and the mice were kept without food but free access to water for another 60 min. The mice were perfused with 30 ml of PBS, and AT and livers were excised, washed, weighed, and frozen at −20°C until further use. Tissues were homogenized in PBS, and the lipids were extracted with $CHCl_3$-methanol (2:1, v/v), followed by a second extraction with n-hexane-isopropanol (3:2, v/v). The unified organic extracts were evaporated under a stream of nitrogen gas and redissolved in 800 μl of ethanol, 100 μl of water, and 240 μl of 50% KOH. After saponification (1 h at 70°C), the solution was acidified with 6 M HCl and lipids were re-extracted with hexane-diethyl ether (1:1, v/v). The extract was washed with water and dried. Extract aliquots were counted in 10 ml of scintillation cocktail (Ultima Gold®, Packard BioScience, CT) in the β-counter.

Glucose uptake into mouse AT

Glucose uptake into ex vivo fat pads was determined after an overnight fasting/2 h refeeding period (induced lipogenesis) according to the methods of Gao and Serrero (10). Epididymal fat pads from L0-MCK and L2 mice were removed surgically and washed in Krebs-Ringer buffer at 37°C. In a 24-well cell culture dish, 50–100 mg pieces of AT were minced with scissors and incubated in 600 μl of Krebs-Ringer buffer containing 1 μCi of [^{14}C]deoxyglucose (New England Nuclear, Boston, MA) at 37°C for 30 min on a rotary shaker. For lysis, tissues were washed thoroughly three times and transferred into 750 μl of 0.5 N sodium hydroxide. Lysate aliquots (150 μl) were counted in 10 ml of scintillation cocktail (Ultima Gold®) in the β-counter, and radioactivity was related to the wet tissue mass.

Enzyme activities

Enzyme activities were determined spectrophotometrically (Beckman DU 500) in AT extracts of fed or overnight fasted animals. Abdominal fat pads were excised, weighed, and shock-frozen in liquid nitrogen. Subsequently, AT was homogenized in 3 vol of cold homogenization buffer (9 mM KH_2PO_4, 85 mM K_2HPO_4, 1 mM DTT, and 70 mM $KHCO_3$, pH 7). After centrifugation for 12 min at 20,000 *g*, the fat cake was discarded and the infranatant was centrifuged at 100,000 *g* for 1 h at 4°C. The supernatant was collected and filtered through cotton tissue to remove the remaining fat. Protein concentrations of the filtrated homogenates were determined by the method of Lowry et al. (11).

Acetyl-CoA carboxylase (ACC) activity was measured using a NADH-linked assay with minor modifications (12). The medium (56 mM Tris-HCl, pH 8, 10 mM $MgCl_2$, 11 mM EDTA, 4 mM ATP, 52 mM $KHCO_3$, 0.75 mg/ml BSA, 0.5 mM NADH, and 1.4 mM phosphoenolpyruvate) was mixed with 5.6 U/ml pyruvate kinase and 5.6 U/ml lactate dehydrogenase. The baseline was followed at 30°C until a constant slope was reached. To 340 μl of medium, 150 μl of activated homogenate were added, and the reaction was started with acetyl-CoA (0.125 mM final concentration). For enzyme activation, equal volumes of the homogenate and activation buffer [20 mM citrate, 100 mM Tris-HCl, pH 8, 1.5 mg/ml BSA, 20 mM $MgCl_2$ and 20 mM GSH, pH 7.5; adapted from refs. (13, 14)] were incubated for 15 min at 37°C.

FA synthase (FAS) enzymatic activity was determined as the decrease of the NADPH absorption at 340 nm (15). ATP-dependent citrate lyase (ATP-CL) was measured using the hydroxamate method (16). As a standard solution, succinic anhydride was prepared as described by Lipmann and Tuttle (17).

Pyruvate dehydrogenase (PDH) activity was measured in the mitochondrial fraction of tissue homogenates. After the ultracentrifugation step (see above), the mitochondrial pellet was resuspended in 110 μl of medium containing 50 mM phosphate buffer, pH 7.5, 0.1% Triton X-100, 1 mM EDTA, and 5 mM sodium dichloroacetate to inhibit PDH kinase (18). The suspension was freeze-thawed and centrifuged at 27,000 *g* for 15 min at 4°C, and the supernatant was activated at 37°C for 10 min. PDH activity was measured by monitoring the increase in *p*-iodonitrotetrazoliumviolet absorption at 500 nm (19).

The NADPH-linked activities of glucose-6-phosphate dehydrogenase (G6PDH) and malic enzyme (ME) were investigated after the increase in absorption at 340 nm. For the determination of G6PDH activity, a buffer containing 50 mM Tris-HCl, pH 8, 1 mM $MgCl_2$, and 5 mM NADP was mixed with 60 μg of cytosolic protein/ml, and the reaction was started with glucose-6-phosphate

acid (8 mM final concentration) at 37°C. ME activity was measured in a buffer containing 50 mM Tris-HCl, pH 7.4, 1 mM $MnCl_2$, 5 mM NADP, and 180 μg protein/ml. The reaction was started with L-malic acid (8 mM final concentration) at room temperature. Glycerolkinase activity was measured after the method of Guan et al. (20).

Analysis of HSL enzyme activity

ATs of fed mice were removed surgically, washed with PBS, and homogenized in 1 ml of lysis buffer containing 0.25% sucrose, 1 mM EDTA, 1 mM dithioerythreitol, 20 μg/ml leupeptin, 2 μg/ml antipain, and 1 μg/ml pepstatin, pH 7.0. as described previously (21). Fat-free infranatants were obtained by centrifugation at 13,000 rpm for 1 h at 4°C and analyzed for enzyme activity. For substrate preparation, 60 μl of triolein solution in chloroform (100 mg/ml), 30 μl of phospholipid solution in chloroform [20 mg/ml phosphatidylcholine-phosphatidylinositol (3:1)], and 50 μl of [^{3}H]triolein (1 mCi/ml) were evaporated under a stream of nitrogen. After the addition of 2 ml of 0.1 M potassium phosphate buffer, pH 7, the mixture was sonicated on ice four times for 1 min each with a 1 min interval between the cycles. Subsequently, 1 ml of potassium phosphate buffer, pH 7, was added, and the sonication was continued two times for 30 s. After sonication, 1 ml of 20% BSA was added, and the final substrate was immediately used for activity determinations. For the enzymatic reaction, 100 μl of substrate was incubated with 100 μl of sample for 30 min at 37°C. The reaction was terminated by the addition of 3.25 ml of extraction solution [methanol-chloroform-*N*-heptane (10:9:7)] and 1 ml of 0.1 M potassium carbonate-boric acid, pH 10.5. The samples were vortexed vigorously for 30 s and centrifuged at 3,000 rpm for 15 min. One milliliter of the aqueous phase was aspirated and counted in 8 ml of scintillation cocktail (Ultima Gold®) in a β-counter. HSL activity was calculated as micromoles of FAs released per hour of incubation time times 100 μg of protein in the homogenate.

RNA isolation and Northern blot analysis

ATs of fed mice were removed surgically, weighed, and subsequently frozen in liquid nitrogen. Total RNA was isolated after homogenization in TRI Reagent (MRC, Karlsruhe, Germany) according to the manufacturer's protocol. For Northern blot analysis, 10 μg of total RNA was separated by 1% formaldehyde agarose gel electrophoresis and blotted overnight onto nylon membranes (Hybond N^+; Amersham Biosciences, Vienna, Austria). RNA was crosslinked to the membrane by ultraviolet irradiation. The blots were prehybridized in hybridization buffer (0.15 M sodium phosphate, pH 7.2, 1 mM EDTA, 7% SDS, and 1% BSA) for 4 h at 65°C. Membranes were hybridized overnight at 65°C in the same buffer with the appropriate radiolabeled probes. The blots were washed in 2× SSC containing 0.1% SDS for 20 min at room temperature, followed by two additional washing steps in 1× SSC containing 0.1% SDS for 10 min at 65°C each. Specific hybridization signals were visualized after exposure to a PhosphorImager Screen on a Storm PhosphorImager (Amersham Biosciences).

To obtain specific DNA probes, cDNA from murine AT was generated by reverse transcription-PCR (Advantage RT-for-PCR Kit; Clontech, Palo Alto, CA). Specific primers for PCR were designed, and PCR products were cloned into a pCR 2.1 vector (Invitrogen, Karlsruhe, Germany): acyl-CoA:diacylglycerol acyltransferase-1 (DGAT-1): forward primer, CTGAGGTGCCATCGTCTGC; reverse primer, CGGCACCACAGGTTGACATC, leptin: forward primer, CAGCTGCAAGGTGCAAGAAG, reverse primer, TGCACATGGCTCTCTTCTCC; SREBP-1: forward primer, GCAAATCACTGAAGGACCTGG; reverse primer, GCTGGTGCAGCTTATGGTAGAC; ACC: forward primer, GCTCTGTACAACGCAGGCAT; reverse primer, AGTCTGTCCAGCCAGCCAGT. For peroxisome proliferator-activated receptor (PPARγ) and stearoyl-CoA desaturase (SCD-2), the cDNA probes were a kind donation of Dr. Levak-Frank. After verification of the DNA sequence, the clones were radioactively labeled with [^{32}P]dCTP (New England Nuclear) using a random priming kit (Prime-a-Gene Kit; Promega, Mannheim, Germany).

Real-time PCR

Quantitative real-time PCR was used to determine the relative levels of lipogenic and glycolytic enzymes. Reverse transcription and PCR were performed according to the manufacturer's instructions (TaqMan™ One Step RT-PCR Kit; Applied Biosystems, Vienna, Austria) on a 5700 AbiPrism Sequence Detection System (Applied Biosystems). Specific primers and TaqMan™ probes were designed using Primer-Express software (Applied Biosystems) to exclude the detection of genomic DNA. Sequence-specific amplification was detected with an increasing fluorescence signal of FAM (reporter dye) during the amplification cycle. Initially, amplifications of murine β-actin and hypoxanthineguanine phosphoribosyl transferase were performed as internal controls for variations in mRNA amounts. As both "housekeeping" genes gave the same normalized quantities, levels of the different mRNAs were finally presented after normalization to murine β-actin mRNA levels. Primers and probes were as follows: mPDH forward, 5′-CACAGTGCTGCCATATTGTAAGC-3′; mPDH reverse, 5′-GCAAGTACAATGGAAAAGATGAGGT-3′; mPDH probe, 5′-CAAAGATCTGACCCTGATTAGCAGCACCA-3′; mβ-actin forward, 5′-GACAGGATGCAGAAGGAGATTACTG-3′; mβ-actin reverse, 5′-GCCACCGATCCACACAGAGT-3′; mβ-actin probe, 5′-CAAGATCATTGCTCCTCCTGAGCGCA-3′; mHPRT forward, 5′-TTGCTCGAGATGTCATGAAGGA-3′; mHPRT reverse, 5′-TGAGAGATCATCTCCACCAATAACTT-3′; mHPRT probe, 5′-TGGGAGGCCATCACATTGTGGC-3′; mG6PDH forward, 5′-GGGCAAAGAGATGGTCCAGA-3′; mG6PDH reverse, 5′-CAATGTTGTCTCGATTCCAGATG-3′; mG6PDH probe, 5′-ATCCTGTTGGCAAACCTCAGCACCA-3′; mFAS forward, 5′-ATGTGAACAGCGCAGGCAC-3′; mFAS reverse, 5′-ACAATGCCCACGTCACCAAT-3′; mFAS probe, 5′-TGTCCTCCCAGGCCTTGCCGT-3′; mATP-CL forward, 5′-TTACGGACAGAGAGCCACACTC-3′; mATP-CL reverse, 5′-CTCTGAAATTGCCTTGGCTGA-3′; mATP-CL probe, 5′-AGAGGTAAACCAGGTCCCTCTGCAGCC-3′; mME forward, 5′-GATTTTGCCAATCGGAATGC-3′; mME reverse, 5′-TTATTCGAAGAGCTGCAAGGAGA-3′; mME probe, 5′-AACCGCAACAGACGCTGTTCCTTAAATAT-3′; mScap forward, 5′-CACCATCACATTGCAACCATCT-3′; mScap reverse, 5′-AACGGTACCAGCCATGATGAG-3′; mScap probe, 5′-CATCTACTTCCTGGCCCGCACTCG-3′; mInsig-1 forward, 5′-CCGGAACACCCATAGCTAACTG-3′; mInsig-1 reverse, 5′-CCTGATTTCCTCTATATCCGTTCTTG-3′; mInsig-1 probe, 5′-CCTATGTTTCCCACTGTGACACCTCCTGA-3′; mInsig-2 forward, 5′-CACTTTTTCCACCAGATGTGATCA-3′; mInsig-2 reverse, 5′-CTCCTAGATGCCTGTCAATGCA-3′; mInsig-2 probe, 5′-ATGCTGCGGCACAGCCTCAGC-3′.

Cell fractionation and immunoblotting

Nuclear extraction was performed as described (22). Protein quantitation was performed after the method of Lowry et al. (11). Aliquots (30 μg of protein) were separated by SDS-PAGE and blotted onto nitrocellulose membranes. For immunoblot analysis, SREBP-1 antibody (Santa Cruz Biotechnology, Heidelberg, Germany) (1:1,000) was visualized with horseradish peroxidase-conjugated goat anti-rabbit IgG (Pierce) (1:10,000) using the Enhanced Chemiluminescence (ECL) Western Blotting Detection System Kit (Amersham Biosciences). Gels were calibrated with the SeeBlue®-prestained molecular weight standard (Invi-

trogen, Lofer, Austria). Membranes were exposed to ECL Hyperfilm (Amersham Biosciences).

Statistical analysis

Results are given as means ± SD. Statistical significance was tested using the two-tailed Student's *t*-test. Significance levels were set at $P < 0.05$, $P \leq 0.01$, and $P \leq 0.001$.

RESULTS

The previous finding of normal fat mass and a lipid composition of mostly saturated and monounsaturated FA (90% vs. 52% in control AT) in chow-fed L0-MCK mice suggested that in the absence of LPL-mediated FA, import adipocytes begin to synthesize FA and TG de novo from carbohydrates. In the present study, we attempted to test this hypothesis and to elucidate the regulatory mechanisms behind this metabolic switch from FA uptake to FA synthesis.

The FA synthesis rate is increased in LPL-deficient AT

Radioactive tracer studies were used to determine the rate of FA production in abdominal AT in the presence (L2) and absence (L0-MCK) of AT-LPL. ^3H_2O was injected into fasted/refed mice, and the radioactivity incorporated into the TG, diglyceride, and nonesterified FA fractions of epididymal fat pads was measured by scintillation counting and compared with the incorporation rate in the liver of both strains. As shown in **Fig. 1A**, the synthesis rate of FAs and their incorporation in neutral lipids was 1.8-fold higher in AT of L0-MCK mice compared with control mice (L2). In contrast, the hepatic production rates of FAs were identical in both mouse strains (Fig. 1B).

Activities and mRNA levels of enzymes involved in the synthesis of FA and TG are increased in LPL-deficient AT

To assess whether the observed increase in the synthesis of FAs was facilitated by the induction of glycolytic and lipogenic pathways, the activities of several relevant enzymes were determined in isolated abdominal fat pads of fed L0-MCK and control mice by spectrophotometric assays (**Table 1**). In the absence of AT-LPL (L0-MCK mice), the catalytic activities of both ACC and FAS in fat pad homogenates were increased by 2.2- and 2.0-fold, respectively, compared with the activities in fat pads from control littermates. Additionally, PDH activity, responsible for mitochondrial acetyl-CoA production, and ATP-CL activity, responsible for the release of acetyl-CoA from citrate in the cytoplasm, were both increased by 98 and 76%, respectively, in L0-MCK mice compared with controls. Finally, the activities of both enzymes that produce NADPH for the synthesis of FAs, G6PDH, and ME were increased by 1.6- and 2.7-fold, respectively, in LPL-deficient AT. In the fasted state, LPL-deficient AT also exhibited a similar trend of increased enzyme activities compared with that in L2 mice. However, the differences were less pronounced and did not reach statistical significance (data not shown).

To assess the supply of glycerolphosphate for TG synthesis in adipocytes, the recently described glycerolkinase activity (20) was measured in AT of fed L0-MCK and control mice. Glycerolkinase activity in AT was found at very low levels that showed no significant differences in mice of both genotypes (Table 1). Adipose glycerolkinase activity represented ~10% of hepatic levels in these animals (data not shown), suggesting that the glycerol backbone of TG is derived mainly from glycolysis or gluconeogenesis.

Consistent with an induction of enzyme activities, the mRNA levels of several enzymes involved in the de novo synthesis of FA were also increased markedly (**Fig. 2**), as was evident from real-time PCR and Northern blot analysis of total AT RNA from both mouse strains. FAS and ATP-CL mRNA levels showed a 2.7- and 5.0-fold increase, respectively, and mRNA concentrations of G6PDH and ME were increased by 2.7- and 2.9-fold, respectively, in AT of L0-MCK mice. Despite the increased enzyme activity, the mRNA levels of ACC and PDH were identical in fat pads of L0-MCK and control mice (Fig. 2). The increased de novo production of FA in LPL-deficient AT was associated with a 6.3-fold increase in the mRNA levels of SCD-2

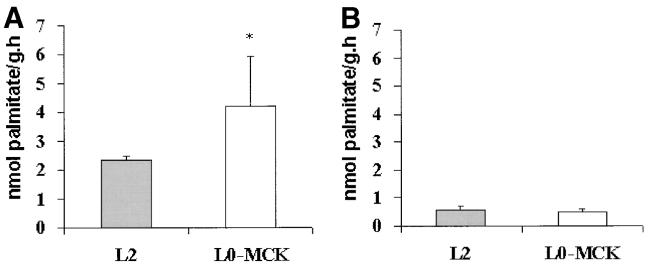

Fig. 1. The rates of fatty acid (FA) biosynthesis in adipose tissue (AT) (A) and liver (B) of control (L2) and AT-lipoprotein lipase (LPL)-deficient (L0-MCK) mice. FA de novo synthesis was measured using ^3H_2O as a tracer. One millicurie of ^3H_2O was injected into the tail vein of overnight fasted and refed mice. One hour later, AT and livers were excised and lipids were extracted with $CHCl_3$-methanol (2:1, v/v) followed by a second extraction with n-hexane-isopropanol (3:2, v/v). The lipids were saponified, and after acidification, the FAs were reextracted and quantitated by liquid scintillation. The values represent means ± SD of experiments using organs from six animals. The asterisk indicates $P < 0.05$.

TABLE 1. Lipogenic enzyme activities in control and adipose tissue-lipoprotein lipase-deficient mice

Enzyme	n	L2	L0-MCK
Acetyl-CoA carboxylase	9	21.1 ± 10.7	46.6 ± 19.3[a]
Fatty acid synthase	9	1.86 ± 0.49	3.75 ± 1.18[a]
Citrate lyase	9	0.25 ± 0.13	0.44 ± 0.14[a]
Pyruvate dehydrogenase	9	13.7 ± 8.34	27.2 ± 12.0[a]
Glucose-6-phosphate dehydrogenase	9	233 ± 56	369 ± 60[b]
Malic enzyme	9	0.067 ± 0.037	0.178 ± 0.093[a]
Glycerolkinase	5	475 ± 73	361 ± 196

Fat pads of fed control (L2) and adipose tissue-lipoprotein lipase (AT-LPL)-deficient (L0-MCK) mice were homogenized on ice in carbonate/phosphate buffer containing DTT. Catalytic enzyme activities were measured as described in Experimental Procedures. Protein concentrations were determined by the method of Lowry et al. (11). Values are given as IU/mg protein ± SD, except those for acetyl-CoA carboxylase (IU/μg protein) and glycerolkinase (cpm/mg protein).

[a] $P < 0.05$ compared with controls.

[b] $P \leq 0.001$ compared with controls.

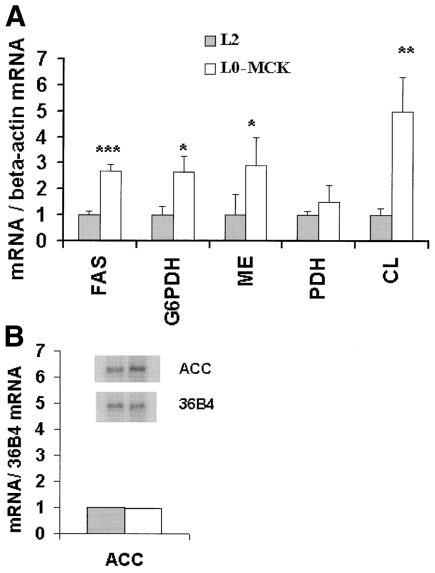

Fig. 2. mRNA concentrations of lipogenic enzymes in AT of control (L2) and AT-LPL-deficient (L0-MCK) mice. Total RNA was isolated from fat pads of fed mice. A: mRNA concentrations were determined by fluorescent real-time PCR on a 5700 AbiPrism Sequence Detection System (Applied Biosystems) using specific TaqMan™ probes. The obtained mRNA concentrations were normalized to β-actin. The values are presented as means ± SD of L2 animals (n = 4; gray bars) and L0-MCK animals (n = 4; white bars). mRNA determinations were performed in triplicate. mRNA levels in L0-MCK mice are presented in relation to the levels in AT of L2 mice (arbitrarily set to 1). CL, citrate lyase; FAS, fatty acid synthase; G6PDH, glucose-6-phosphate dehydrogenase; ME, malic enzyme; PDH, pyruvate dehydrogenase. Single asterisk, $P < 0.05$; double asterisk, $P \leq 0.01$; triple asterisk, $P \leq 0.001$. B: Acetyl-CoA carboxylase (ACC) mRNA levels were quantitated by Northern blot analysis of total AT RNA. After hybridization with a ^{32}P-labeled specific ACC cDNA probe, the blots were subjected to autoradiography, and signal intensities were quantified on a Storm PhosphorImager with ImageQuant software. Specific signals were normalized to the concentration of 36B4 mRNA. mRNA levels in L0-MCK mice (n = 2; white bar) are presented in relation to the levels in AT of L2 mice (n = 2; gray bar) (arbitrarily set to 1).

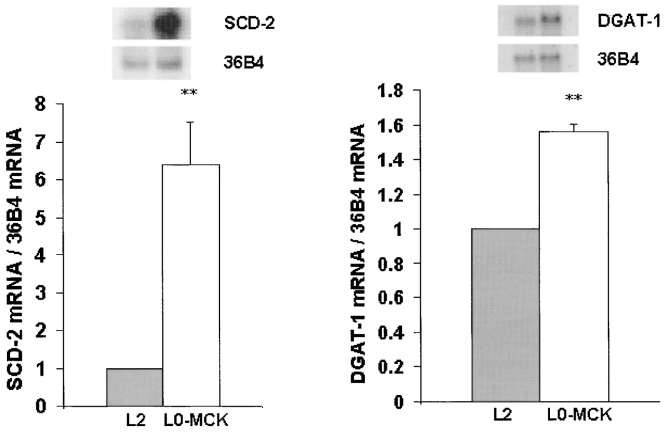

Fig. 3. mRNA concentrations of stearoyl-CoA desaturase-2 (SCD-2) and acyl-CoA:diacylglycerol acyltransferase-1 (DGAT-1) in AT of control (L2) and AT-LPL-deficient (L0-MCK) mice. Total RNA was isolated from fat pads of fed L2 and L0-MCK mice. Ten micrograms of total RNA were separated on a formaldehyde agarose gel and blotted onto a nylon membrane. After hybridization with ^{32}P-labeled specific murine SCD-2 and DGAT-1 cDNA probes, the blots were subjected to autoradiography, and signal intensities were quantified on a Storm PhosphorImager with ImageQuant software. Specific signals were normalized to the concentration of 36B4 mRNA. mRNA levels in L0-MCK mice (n = 2; white bars) are presented as means ± SD in relation to the levels in AT of L2 mice (n = 2; gray bars) (arbitrarily set to 1). Double asterisk, $P \leq 0.01$.

and a 1.6-fold increase of the mRNA concentration of DGAT-1 in fat pads of L0-MCK mice (**Fig. 3**).

HSL-mediated lipolysis is not reduced in LPL-deficient AT

Because HSL is an important enzyme for the hydrolysis of TG in AT, we examined whether reduced HSL activity accounted for the maintenance of normal fat mass in L0-MCK mice. HSL enzyme activity was found to be moderately increased (80%) in LPL-deficient AT compared with control AT (**Fig. 4**), whereas HSL mRNA levels were not significantly different (Fig. 4, inset).

The uptake and use of glucose is increased in LPL-deficient AT

Because plasma glucose represents a major substrate for endogenous lipogenesis, the use of glucose in AT was measured by the determination of the uptake rates of [^{14}C]deoxyglucose in isolated fat pads of L0-MCK and control mice. The net influx of glucose into fat pads of L0-MCK mice was increased, as shown by the 1.8-fold increased uptake of [^{14}C]deoxyglucose in LPL-deficient abdominal fat pads (**Fig. 5**).

The plasma parameters of glucose metabolism are summarized in **Table 2**. The analysis of glucose levels in the fed state (blood taken between 9 and 10 AM) revealed significantly increased concentrations in L0-MCK mice (211 ± 30 mg/dl) compared with control mice (164 ± 41 mg/dl), whereas no significant differences were observed in the fasted state. When inducing lipogenesis by overnight fasting and subsequent refeeding, the blood glucose levels decreased significantly in L0-MCK mice (166 ± 9 mg/dl) but remained high in L2 mice (213 ± 3 mg/dl), indicating an enhanced plasma glucose clearance in L0-MCK mice. Plasma insulin and glucagon levels were determined by radioimmunoassays from blood samples drawn in fasted or fasted/refed conditions. Fasted values of both plasma insulin and glucagon were not significantly different in AT-LPL-deficient and control mice (data not shown). After refeeding, however, plasma insulin levels of L0-MCK mice were 1.9-fold higher than those in control mice, whereas glucagon concentrations were unchanged. Accordingly, the molar ratio of insulin to glucagon was increased by 2.3-fold in fasted/refed L0-MCK mice compared with control mice. Free FA plasma concentrations showed no significant differences between the genotypes, either in the fasted or in the fed or fasted/refed condition.

Leptin mRNA and protein levels are reduced in LPL-deficient AT

As leptin has been shown to be regulated by both intracellular FA concentrations (23, 24) and SREBP-1 activa-

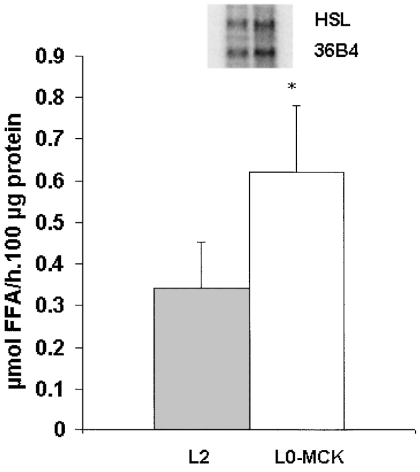

Fig. 4. Hormone-sensitive lipase (HSL) enzyme activities and mRNA concentrations in AT of control (L2) and AT-LPL-deficient (L0-MCK) mice. For HSL activity determinations, abdominal fat pads were excised, washed in PBS, and homogenized in lysis buffer. After centrifugation, 100 µl fat-free aliquots from the infranatant were incubated with 100 µl of [^{3}H]triolein substrate. Subsequently, the released FAs were separated from other lipids by alkaline extraction and quantitated by liquid scintillation counting. The activity values are presented as means ± SD of L2 animals (n = 5; gray bar) and L0-MCK animals (n = 5; white bar). The asterisk indicates $P < 0.05$. In the inset, 10 µg of total RNA was separated on a formaldehyde agarose gel and blotted onto a nylon membrane. After hybridization with a ^{32}P-labeled specific murine HSL cDNA probe, the blots were subjected to autoradiography. Specific signals were normalized to the concentration of 36B4 mRNA. FFA, free FA.

tion (25), leptin mRNA and plasma protein levels were analyzed in L0-MCK and L2 mice (**Fig. 6**). In fed mice, Northern blotting experiments revealed a 42% reduction of leptin mRNA expression in AT of L0-MCK mice (Fig. 6A). Leptin protein levels were determined in the plasma of fasted (basal levels) and fasted/refed mice. Basal levels showed no significant differences between L0-MCK and

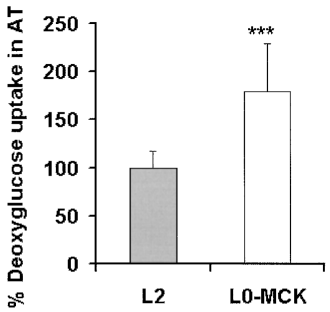

Fig. 5. 2-Deoxyglucose uptake into fat pads of control (L2) and AT-LPL-deficient (L0-MCK) mice. Mice were fasted overnight and refed for 2 h to induce lipogenesis. Abdominal fat pads were excised and incubated in Krebs-Ringer buffer containing [^{14}C]deoxyglucose. After washing and tissue lysis, cell-associated radioactivity was determined by liquid scintillation counting. The values present means ± SD of L2 mice (n = 8, grey bar) and L0-MCK mice (n = 6, white bar). Counts/min.mg of AT from L2 mice were set to 100% glucose uptake. Triple asterisk, $P \leq 0.001$.

TABLE 2. Plasma parameters of glucose metabolism

Parameter	L2 (n = 10)	L0-MCK (n = 5)
Insulin (ng/ml plasma)	0.6 ± 0.23	1.11 ± 0.30[a]
Glucagon (pg/ml plasma)	89.1 ± 28.5	69.7 ± 13.2
Insulin-glucagon (mol/mol)	4.1	9.6
Glucose (mg/dl)		
Fed	164 ± 41	211 ± 30[a]
Fasted	137 ± 21	179 ± 25
Fasted/refed	213 ± 3	166 ± 9[a]
Free fatty acids (mg/dl)		
Fed	7.2 ± 3.4	9.9 ± 3.6
Fasted	11.9 ± 3.5	14.9 ± 6.4
Fasted/refed	10.0 ± 3.8	11.9 ± 3.1

Blood was taken in the morning from control (L2) and AT-LPL-deficient (L0-MCK) mice that had fasted overnight and were refed for 2 h (fasted/refed). Plasma glucose and fatty acid concentrations were also determined from blood samples taken from fed mice and from mice that had fasted overnight (fasted). Plasma insulin and glucagon concentrations were measured by radioimmunoassays, and glucose and fatty acid concentrations were measured enzymatically. Values represent means ± SD.

[a] $P \leq 0.01$ compared with the controls.

L2 mice. In contrast, after fasting and refeeding, the plasma leptin concentrations in L0-MCK animals were 34% lower than those in control littermates (3.8 ± 1.1 vs. 5.8 ± 1.2 ng/ml plasma, respectively) (Fig. 6B).

SREBP-1 and insulin-induced gene-1 expression levels are induced in LPL-deficient AT

To study the effects of limited FA uptake on FA-activated transcription factors in LPL-deficient AT, the mRNA levels of SREBP-1 and PPARγ were examined in isolated fat pads from L0-MCK and L2 mice. Northern blot analysis revealed a 4.5-fold induction of SREBP-1 mRNA levels in LPL-deficient AT (**Fig. 7A**), whereas mRNA levels of PPARγ were slightly but not significantly reduced in fat pads of L0-MCK mice compared with control AT (data not shown). Additionally, Western blot analysis of cytosolic fractions and nuclear extracts revealed that the abundance of both the cytosolic protein and the processed and transcriptionally active 68 kDa nuclear isoform of SREBP-1 were increased by approximately 2-fold in LPL-deficient AT compared with control AT (Fig. 7B). SREBP-1 activation was accompanied by induction of the expression of insulin-induced gene-1 (INSIG-1) and INSIG-2 in AT of L0-MCK mice, as revealed by the 2.8- and 1.4-fold increases of the respective mRNA levels in real-time PCR analysis (**Fig. 8**). The expression of SREBP cleavage-activating protein, an important factor for SREBP translocation from the endoplasmic reticulum to the Golgi, was not different in AT of the two mouse genotypes (Fig. 8).

DISCUSSION

We demonstrated in an earlier study that the absence of LPL in AT of mice that express LPL exclusively in muscle causes an adipose-specific defect in the hydrolysis of TG-rich lipoproteins, decreased FA uptake, and low tissue levels of essential polyunsaturated FAs (5, 6, 26). Unexpect-

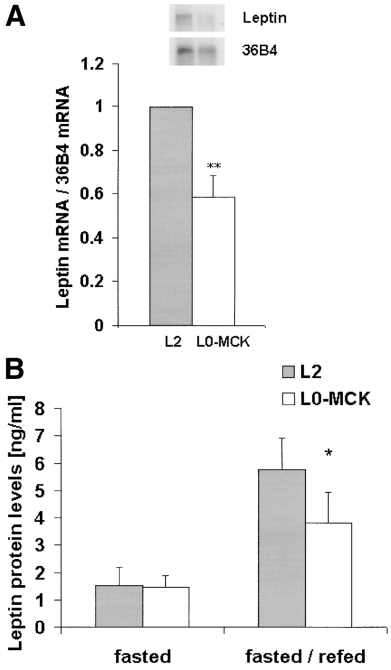

Fig. 6. Leptin mRNA levels in AT and plasma leptin concentrations in control (L2) and AT-LPL-deficient (L0-MCK) mice. A: Total RNA was isolated from fat pads of overnight fasted/refed mice. Ten micrograms of total RNA was separated on a formaldehyde-agarose gel and blotted onto a nylon membrane. After hybridization with a ^{32}P-labeled specific murine leptin cDNA probe, the blots were subjected to autoradiography, and signal intensities were quantified on a Storm PhosphorImager with ImageQuant software. Specific signals were normalized to the concentration of 36B4 mRNA. Leptin mRNA levels in L0-MCK mice (n = 2; white bar) are presented in relation to the levels in AT of L2 mice (n = 2; gray bar) (arbitrarily set to 1). B: Plasma leptin concentrations of overnight fasted and overnight fasted/refed mice were determined using a radioimmunoassay (Linco). The values represent means ± SD of L2 animals (n = 5; gray bars) and L0-MCK mice (n = 5; white bars). Leptin concentrations in plasma were determined in duplicate. Single asterisk, $P < 0.05$; double asterisk, $P \leq 0.01$.

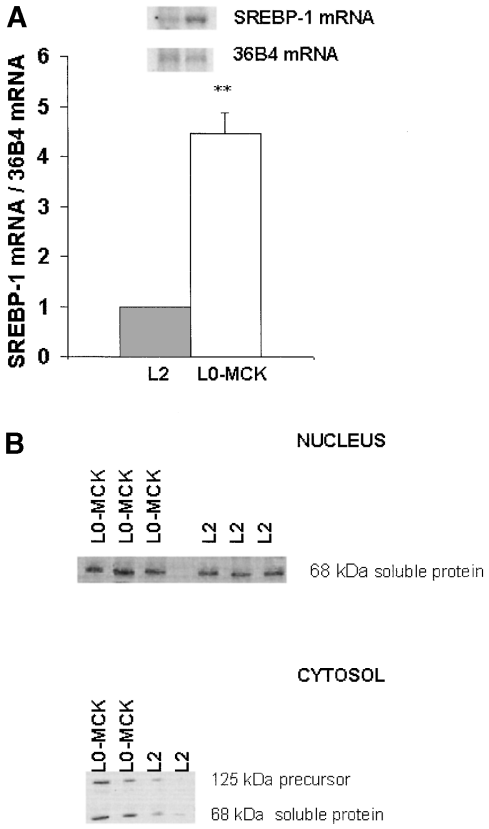

Fig. 7. Sterol regulatory element-binding protein-1 (SREBP-1) mRNA (A) and protein (B) concentrations in AT of control (L2) and AT-LPL-deficient (L0-MCK) mice. A: Ten micrograms of total RNA were separated on a formaldehyde agarose gel and blotted onto a nylon membrane. After hybridization with a ^{32}P-labeled specific murine SREBP-1 cDNA probe (detecting both SREBP-1a and SREBP-1c), the blots were subjected to autoradiography, and signal intensities were quantified on a Storm PhosphorImager with ImageQuant software. Specific signals were normalized to the concentration of 36B4 mRNA. SREBP-1 mRNA levels in L0-MCK mice (n = 2; white bar) are presented as means ± SD in relation to the levels in AT of L2 mice (n = 2; gray bar) (arbitrarily set to 1). Double asterisk, $P \leq 0.01$. B: SREBP-1 protein levels in nuclear extracts and cytosolic fractions of AT. Thirty micrograms of total protein from nuclear extracts or cytosolic fractions were separated by SDS-PAGE, blotted onto a nitrocellulose membrane, and subjected to immunoblot analysis with a SREBP-1 antibody. Bands were visualized using horseradish peroxidase-labeled goat anti-rabbit IgG and enhanced chemiluminescence detection.

edly, however, the total AT mass in these animals was similar to that of mice that expressed LPL normally in AT. Recently, a comparable adipose-specific phenotype was reported in humans affected with type I hyperlipoproteinemia, the familiar deficiency of LPL (27). These observations led to the working hypothesis for our current study, namely, that normal fat mass in AT-LPL-deficient mice was maintained by the induction of intracellular FA and TG synthesis.

In this report, we show that the synthesis of both FA and TG is increased in LPL-deficient AT. In contrast, hepatic FA and TG synthesis are not affected. The upregulation of the rate of FA synthesis is paralleled by an increase in the catalytic activities of enzymes contributing to the biosynthetic pathways of FAs. Increased activities were found for the key enzymes ACC and FAS, the enzymes responsible for the mitochondrial and cytoplasmic production of acetyl-CoA, PDH, and ATP-CL, and the enzymes involved in the production of NADPH, G6PDH, and ME. The expression of SCD-2, the major enzyme responsible for the biosynthesis of palmitoleic acid and oleic acid from saturated precursors, was also markedly induced. This observation explains the increased level of palmitoleic acid in LPL-deficient AT, which is 3.5-fold higher than that in AT that expresses normal amounts of LPL (5). Finally, mRNA levels for the key enzyme in the terminal esterification step of TG synthesis, DGAT-1 (28), were also induced in LPL-deficient AT.

To assess whether the downregulation of HSL and a concomitant reduction of AT lipolysis contributed to the maintenance of fat in LPL-deficient AT, both enzyme activity and mRNA levels of HSL were determined in mice of both genotypes. HSL activity was increased in L0-MCK

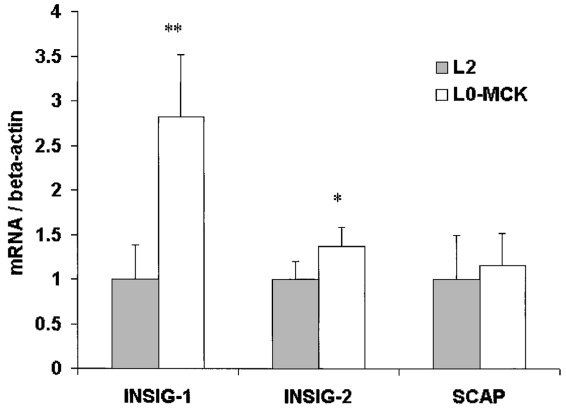

Fig. 8. mRNA concentrations of insulin-induced gene-1 (INSIG-1), INSIG-2, and SREBP cleavage-activating protein (SCAP) in AT of control (L2) and AT-LPL-deficient (L0-MCK) mice. Total RNA was isolated from fat pads of fed mice. mRNA concentrations were determined by fluorescent real-time PCR on a 5700 AbiPrism Sequence Detection System (Applied Biosystems) using specific TaqMan™ probes. The obtained mRNA concentrations were normalized to β-actin. The values are presented as means ± SD of L2 animals (n = 4; gray bars) and L0-MCK animals (n = 4; white bars). mRNA determinations in AT samples were performed in triplicate. mRNA levels in L2-MCK mice are presented in relation to the levels in AT of L2 mice (arbitrarily set to 1). Single asterisk, $P < 0.05$; double asterisk, $P \leq 0.001$.

mice, whereas HSL mRNA levels were similar in L0-MCK and control mice. Accordingly, a compensatory decrease of HSL-mediated lipolysis to retain fat in AT does not occur, consistent with the normal plasma FA levels found in L0-MCK mice.

To investigate whether the requirement of a metabolic substrate for FA synthesis in LPL-deficient AT was met by glucose, several parameters of carbohydrate metabolism were analyzed in mice of both genotypes. The uptake and accumulation of the undegradable derivative 2-deoxyglucose was increased in AT when LPL was absent, and the analysis of plasma glucose concentrations in L0-MCK and control mice during fasting/refeeding experiments suggested that glucose utilization was increased in LPL-deficient AT. These observations are consistent with the view that the substrate required for the de novo synthesis of FA in LPL-deficient AT is provided by increased glucose uptake. Conversely, the transgenic overexpression of LPL in skeletal muscle was shown to be associated with increased TG hydrolysis, increased FA uptake, the accumulation of lipid droplets, impaired glucose usage in myocytes, and muscle-specific insulin resistance (29–32). These findings provide strong evidence that the expression level of LPL in a given tissue directly affects glucose uptake and utilization. Moreover, it is well established that the availability of dietary glucose affects the substrate usage for lipogenesis in AT (33). Hepatic (34) and adipocyte (35, 36) FA de novo synthesis is regulated by the abundance of glucose-6-phosphate and insulin after a carbohydrate-rich diet. Accordingly, the excessive uptake of glucose in AT of transgenic mice overexpressing the insulin-dependent glucose transporter GLUT-4 (37) results in a marked induction of endogenous lipid synthesis and the development of obesity.

To elucidate the regulatory mechanisms behind the metabolic switch from FA uptake to FA synthesis in LPL-deficient AT, the concentrations of relevant hormones and the expression of transcription factors were analyzed. Mice lacking LPL in AT exhibited increased plasma insulin concentrations, decreased leptin levels, and essentially unchanged glucagon concentrations in a lipogenesis-induced state (fasted/refed). Increased insulin levels and an increased insulin-glucagon ratio are consistent with the observed increased uptake of glucose in LPL-deficient AT. It is well established that in the liver, insulin signaling and increased glucose uptake induce SREBP-1 expression and its posttranslational processing (38, 39). In LPL-deficient AT, both SREBP-1 mRNA concentrations and the amount of the nuclear isoform of SREBP-1 were increased, suggesting that insulin and glucose stimulate the transcriptional activity of SREBP-1 in AT as in hepatic tissues. Furthermore, the presence of sterol-responsive elements in the regulatory sequences for genes encoding ACC, FAS, FA elongase, SCD-2, glycerol-3-phosphate acyltransferase, ME, G6PDH, and ATP-CL and the previous data demonstrating that these genes are transcriptionally regulated by SREBP-1 (25) suggested that the induction of lipogenesis in AT when LPL is absent was mediated by SREBP-1.

To gain further insights into the functional role of SREBP-1 in LPL-deficient AT, we studied its effect on targets not directly involved in lipogenesis, the INSIG proteins. INSIG proteins are located in the endoplasmic reticulum. Complex formation with INSIG proteins prevents SREBP cleavage-activating protein and SREBP from progressing to the Golgi apparatus and further processing by site 1 and site 2 proteases (40, 41). Currently, three INSIG isoforms (INSIG-1, INSIG-2a, and INSIG-2b) are known (42, 43). INSIG-1 and INSIG-2b are expressed in a wide variety of tissues, but only INSIG-1 has been shown to be a target of SREBP-1 regulation in cultured cell lines such as CHO cells. INSIG-2a represents a splice variant of INSIG-2b and is found exclusively in the liver. Our data show that both INSIG-1 and -2 are present in AT. INSIG-1 mRNA levels were markedly induced in LPL-deficient AT, whereas INSIG-2 was only moderately increased. INSIG-1 expression in AT was strongly correlated with SREBP-1 mRNA and protein levels in a manner similar to that observed in hepatocytes (40). Although the exact mechanism of INSIG function remains to be elucidated, it is believed that increased INSIG-1 expression in response to SREBP-1 activation counterbalances excessive SREBP-1 action (42). According to our results, such a mechanism appears to be active in both liver and AT.

The plasma leptin concentration as well as leptin mRNA levels in AT were decreased in mice that lacked LPL in AT. In accordance with previous studies demonstrating that leptin represses SREBP-1 expression and, concomitantly, the expression of a cluster of SREBP-1-regulated target genes (including ATP-CL, FAS, ME, and PDH) (44–46), it is likely that both increased insulin and decreased leptin levels coordinately induce lipogenesis in

LPL-deficient AT via SREBP-1. In a recent study, Cohen et al. (47) demonstrated that the lack of leptin in *ob/ob* mice derepresses the expression of SCD-1, which leads to excessive lipid accumulation in AT. Conversely, the lack of SCD-1 has been demonstrated to protect mice against adiposity (48). In accordance with these observations, we show in this study that the lack of LPL in AT is associated with decreased leptin levels and increased SREBP-1 expression, which cause the induction of SCD expression and the induction of lipogenesis.

To date, most studies addressing the role of FAs in gene regulation involved cell culture experiments or feeding various types of FAs to laboratory animals (49–54). With the availability of mice that express LPL exclusively in muscle, it was possible to study the effects of polyunsaturated FA deprivation in AT and the respective metabolic adaptations in vivo. Taken together, the results from this study suggest the following model. The absence of LPL in AT and the concomitant overexpression of LPL in muscle cause increased insulin levels in plasma. Increased insulin levels lead to increased glucose uptake in AT and decreased leptin expression. High insulin, low leptin, increased glucose uptake, and decreased availability of nutritional FAs are able to activate SREBP-1 expression and processing, which in turn leads to the transcriptional induction of lipogenesis. The ultimate outcome of this upregulation is a compensatory synthesis of lipids and the maintenance of AT mass.

This work was supported by Spezialforschungsbereich Biomembranes provided by Austrian Fonds zur Förderung der Wissenschaftlichen Forschung grants F00701 and F00713, by the Genomforschung in Österreich Project Genomics of Lipid-associated Disorders provided by the Austrian Federal Ministry of Education, Science, and Culture, and by Austrian FWF grant 15.358-Med. The authors thank Martina Brtnik for excellent technical assistance, Astrid Hermann for help with the mice, and Ellen Zechner for critically reviewing the manuscript.

REFERENCES

1. Merkel, M., R. H. Eckel, and I. J. Goldberg. 2002. Lipoprotein lipase: genetics, lipid uptake, and regulation. *J. Lipid Res.* **43:** 1997–2006.
2. Preiss-Landl, K., R. Zimmermann, G. Hammerle, and R. Zechner. 2002. Lipoprotein lipase: the regulation of tissue specific expression and its role in lipid and energy metabolism. *Curr. Opin. Lipidol.* **13:** 471–481.
3. Kraemer, F. B., and W. J. Shen. 2002. Hormone-sensitive lipase: control of intracellular tri-(di-)acylglycerol and cholesteryl ester hydrolysis. *J. Lipid Res.* **43:** 1585–1594.
4. Haemmerle, G., R. Zimmermann, and R. Zechner. 2003. Letting lipids go: hormone-sensitive lipase. *Curr. Opin. Lipidol.* **14:** 289–297.
5. Weinstock, P. H., S. Levak-Frank, L. C. Hudgins, H. Radner, J. M. Friedman, R. Zechner, and J. L. Breslow. 1997. Lipoprotein lipase controls fatty acid entry into adipose tissue, but fat mass is preserved by endogenous synthesis in mice deficient in adipose tissue lipoprotein lipase. *Proc. Natl. Acad. Sci. USA.* **94:** 10261–10266.
6. Levak-Frank, S., P. H. Weinstock, T. Hayek, R. Verdery, W. Hofmann, R. Ramakrishnan, W. Sattler, J. L. Breslow, and R. Zechner. 1997. Induced mutant mice expressing lipoprotein lipase exclusively in muscle have subnormal triglycerides yet reduced high density lipoprotein cholesterol levels in plasma. *J. Biol. Chem.* **272:** 17182–17190.
7. Cryer, A. 1985. Lipoprotein lipase and the uptake of lipids by adipose cells during development. *Reprod. Nutr. Dev.* **25:** 255–270.
8. Rogers, M. P., and D. S. Robinson. 1974. Effects of cold exposure on heart clearing factor lipase and triglyceride utilization in the rat. *J. Lipid Res.* **15:** 263–272.
9. Lowenstein, J. M. 1971. Effect of (−)-hydroxycitrate on fatty acid synthesis by rat liver in vivo. *J. Biol. Chem.* **246:** 629–632.
10. Gao, J., and G. Serrero. 1999. Adipose differentiation related protein (ADRP) expressed in transfected COS-7 cells selectively stimulates long chain fatty acid uptake. *J. Biol. Chem.* **274:** 16825–16830.
11. Lowry, O. H., N. J. Rosebrough, A. L. Farr, and R. J. Randall. 1951. Protein measurement with the Folin phenol reagent. *J. Biol. Chem.* **193:** 265–275.
12. Matsuhashi, M., S. Matsuhashi, S. Numa, and F. Lynen. 1964. Zur Biosynthese der Fettsäuren. IV. Acetyl-CoA Carboxylase aus Hefe. *Biochem. Z.* **340:** 243–262.
13. Inoue, H., and J. M. Lowenstein. 1975. Acetyl coenzyme A carboxylase from rat liver. EC 6.4.1.2 acetyl-CoA:carbon dioxide ligase (ADP). *Methods Enzymol.* **35:** 3–11.
14. Tanabe, T., S. Nakanishi, T. Hashimoto, H. Ogiwara, J. Nikawa, and S. Numa. 1981. Acetyl-CoA carboxylase from rat liver. *Methods Enzymol.* **71 Pt C:** 5–16.
15. Nepokroeff, C. M., M. R. Lakshmanan, and J. W. Porter. 1975. Fatty-acid synthase from rat liver. *Methods Enzymol.* **35:** 37–44.
16. Takeda, Y., F. Suzuki, and H. Inoue. 1969. ATP citrate lyase (citrate-cleavage enzyme). *Methods Enzymol.* **13:** 153–160.
17. Lipmann, F., and L. C. Tuttle. 1945. A specific micromethod for the determination of PDHC activity in cultured human fibroblasts. *J. Biochem. Biophys. Methods.* **100:** 21–28.
18. Sorbi, S., and J. P. Blass. 1981. Spectrophotometric measurement of pyruvate dehydrogenase complex activity in cultured human fibroblasts. *J. Biochem. Biophys.* **5:** 169–176.
19. Hinman, L. M., and J. P. Blass. 1981. An NADH-linked spectrophotometric assay for pyruvate dehydrogenase complex in crude tissue homogenates. *J. Biol. Chem.* **256:** 6583–6586.
20. Guan, H. P., Y. Li, M. V. Jensen, C. B. Newgard, C. M. Steppan, and M. A. Lazar. 2002. A futile metabolic cycle activated in adipocytes by antidiabetic agents. *Nat. Med.* **8:** 1122–1128.
21. Holm, C., and T. Osterlund. 1999. Hormone-sensitive lipase and neutral cholesteryl ester lipase. *In* Lipase and Phospholipase Protocols. M. H. Doolittle and K. Reue, editors. Humana Press, Totowa, NJ. 109–121.
22. Wang, X., R. Sato, M. S. Brown, X. Hua, and J. L. Goldstein. 1994. SREBP-1, a membrane-bound transcription factor released by sterol-regulated proteolysis. *Cell.* **77:** 53–62.
23. Cha, M. C., and P. J. Jones. 1998. Dietary fat type and energy restriction interactively influence plasma leptin concentration in rats. *J. Lipid Res.* **39:** 1655–1660.
24. Reseland, J. E., F. Haugen, K. Hollung, K. Solvoll, B. Halvorsen, I. R. Brude, M. S. Nenseter, E. N. Christiansen, and C. A. Drevon. 2001. Reduction of leptin gene expression by dietary polyunsaturated fatty acids. *J. Lipid Res.* **42:** 743–750.
25. Horton, J. D., J. L. Goldstein, and M. S. Brown. 2002. SREBPs: activators of the complete program of cholesterol and fatty acid synthesis in the liver. *J. Clin. Invest.* **109:** 1125–1131.
26. Levak-Frank, S., W. Hofmann, P. H. Weinstock, H. Radner, W. Sattler, J. L. Breslow, and R. Zechner. 1999. Induced mutant mouse lines that express lipoprotein lipase in cardiac muscle, but not in skeletal muscle and adipose tissue, have normal plasma triglyceride and high-density lipoprotein-cholesterol levels. *Proc. Natl. Acad. Sci. USA.* **96:** 3165–3170.
27. Ullrich, N. F., J. Q. Purnell, and J. D. Brunzell. 2001. Adipose tissue fatty acid composition in humans with lipoprotein lipase deficiency. *J. Invest. Med.* **49:** 273–275.
28. Cases, S., S. J. Smith, Y. W. Zheng, H. M. Myers, S. R. Lear, E. Sande, S. Novak, C. Collins, C. B. Welch, A. J. Lusis, S. K. Erickson, and R. V. J. Farese. 1998. Identification of a gene encoding an acyl CoA:diacylglycerol acyltransferase, a key enzyme in triacylglycerol synthesis. *Proc. Natl. Acad. Sci. USA.* **95:** 13018–13023.
29. Levak-Frank, S., H. Radner, A. Walsh, R. Stollberger, G. Knipping, G. Hoefler, W. Sattler, P. H. Weinstock, J. L. Breslow, and R. Zechner. 1995. Muscle-specific overexpression of lipoprotein lipase causes a severe myopathy characterized by proliferation of mitochondria and peroxisomes in transgenic mice. *J. Clin. Invest.* **96:** 976–986.

30. Kim, J. K., J. J. Fillmore, Y. Chen, C. Yu, I. K. Moore, M. Pypaert, E. P. Lutz, Y. Kako, W. Velez-Carrasco, I. J. Goldberg, J. L. Breslow, and G. I. Shulman. 2001. Tissue-specific overexpression of lipoprotein lipase causes tissue-specific insulin resistance. *Proc. Natl. Acad. Sci. USA.* **98:** 7522–7527.
31. Ferreira, L. D., L. K. Pulawa, D. R. Jensen, and R. H. Eckel. 2001. Overexpressing human lipoprotein lipase in mouse skeletal muscle is associated with insulin resistance. *Diabetes.* **50:** 1064–1068.
32. Voshol, P. J., M. C. Jong, V. E. Dahlmans, D. Kratky, S. Levak-Frank, R. Zechner, J. A. Romijn, and L. M. Havekes. 2001. In muscle-specific lipoprotein lipase-overexpressing mice, muscle triglyceride content is increased without inhibition of insulin-stimulated whole-body and muscle-specific glucose uptake. *Diabetes.* **50:** 2585–2590.
33. Foufelle, F., J. Girard, and P. Ferre. 1996. Regulation of lipogenic enzyme expression by glucose in liver and adipose tissue: a review of the potential cellular and molecular mechanisms. *Adv. Enzyme Regul.* **36:** 199–226.
34. Koo, S. H., A. K. Dutcher, and H. C. Towle. 2001. Glucose and insulin function through two distinct transcription factors to stimulate expression of lipogenic enzyme genes in liver. *J. Biol. Chem.* **276:** 9437–9445.
35. Towle, H. C., E. N. Kaytor, and H. M. Shih. 1997. Regulation of the expression of lipogenic enzyme genes by carbohydrate. *Annu. Rev. Nutr.* **17:** 405–433.
36. Girard, J., P. Ferre, and F. Foufelle. 1997. Mechanisms by which carbohydrates regulate expression of genes for glycolytic and lipogenic enzymes. *Annu. Rev. Nutr.* **17:** 325–352.
37. Shepherd, P. R., L. Gnudi, E. Tozzo, H. Yang, F. Leach, and B. B. Kahn. 1993. Adipose cell hyperplasia and enhanced glucose disposal in transgenic mice overexpressing GLUT4 selectively in adipose tissue. *J. Biol. Chem.* **268:** 22243–22246.
38. Shimano, H. 2001. Sterol regulatory element-binding proteins (SREBPs): transcriptional regulators of lipid synthetic genes. *Prog. Lipid Res.* **40:** 439–452.
39. Foufelle, F., and P. Ferre. 2002. New perspectives in the regulation of hepatic glycolytic and lipogenic genes by insulin and glucose: a role for the transcription factor sterol regulatory element binding protein-1c. *Biochem. J.* **366:** 377–391.
40. Yang, T., P. J. Espenshade, M. E. Wright, D. Yabe, Y. Gong, R. Aebersold, J. L. Goldstein, and M. S. Brown. 2002. Crucial step in cholesterol homeostasis: sterols promote binding of SCAP to INSIG-1, a membrane protein that facilitates retention of SREBPs in ER. *Cell.* **110:** 489–500.
41. Gimpl, G., K. Burger, and F. Fahrenholz. 2002. A closer look at the cholesterol sensor. *Trends Biochem. Sci.* **27:** 596–599.
42. Yabe, D., M. S. Brown, and J. L. Goldstein. 2002. Insig-2, a second endoplasmic reticulum protein that binds SCAP and blocks export of sterol regulatory element-binding proteins. *Proc. Natl. Acad. Sci. USA.* **99:** 12753–12758.
43. Yabe, D., R. Komuro, G. Liang, J. L. Goldstein, and M. S. Brown. 2003. Liver-specific mRNA for Insig-2 down-regulated by insulin: implications for fatty acid synthesis. *Proc. Natl. Acad. Sci. USA.* **100:** 3155–3160.
44. Soukas, A., N. D. Socci, B. D. Saatkamp, S. Novelli, and J. M. Friedman. 2001. Distinct transcriptional profiles of adipogenesis in vivo and in vitro. *J. Biol. Chem.* **276:** 34167–34174.
45. Liang, C. P., and A. R. Tall. 2001. Transcriptional profiling reveals global defects in energy metabolism, lipoprotein, and bile acid synthesis and transport with reversal by leptin treatment in ob/ob mouse liver. *J. Biol. Chem.* **276:** 49066–49076.
46. Nadler, S. T., J. P. Stoehr, K. L. Schueler, G. Tanimoto, B. S. Yandell, and A. D. Attie. 2000. The expression of adipogenic genes is decreased in obesity and diabetes mellitus. *Proc. Natl. Acad. Sci. USA.* **97:** 11371–11376.
47. Cohen, P., M. Miyazaki, N. D. Socci, A. Hagge-Greenberg, W. Liedtke, A. A. Soukas, R. Sharma, L. C. Hudgins, J. M. Ntambi, and J. M. Friedman. 2002. Role for stearoyl-CoA desaturase-1 in leptin-mediated weight loss. *Science.* **297:** 240–243.
48. Ntambi, J. M., M. Miyazaki, J. P. Stoehr, H. Lan, C. M. Kendziorski, B. S. Yandell, Y. Song, P. Cohen, J. M. Friedman, and A. D. Attie. 2002. Loss of stearoyl-CoA desaturase-1 function protects mice against adiposity. *Proc. Natl. Acad. Sci. USA.* **99:** 11482–11486.
49. Price, P. T., C. M. Nelson, and S. D. Clarke. 2000. Omega-3 polyunsaturated fatty acid regulation of gene expression. *Curr. Opin. Lipidol.* **11:** 3–7.
50. Jump, D. B., S. D. Clarke, A. Thelen, and M. Liimatta. 1994. Coordinate regulation of glycolytic and lipogenic gene expression by polyunsaturated fatty acids. *J. Lipid Res.* **35:** 1076–1084.
51. Baillie, R. A., D. B. Jump, and S. D. Clarke. 1996. Specific effects of polyunsaturated fatty acids on gene expression. *Curr. Opin. Lipidol.* **7:** 53–55.
52. Iritani, N., H. Fukuda, and K. Tada. 1996. Nutritional regulation of lipogenic enzyme gene expression in rat epididymal adipose tissue. *J. Biochem.* **120:** 242–248.
53. Raclot, T., R. Groscolas, D. Langin, and P. Ferre. 1997. Site-specific regulation of gene expression by n-3 polyunsaturated fatty acids in rat white adipose tissues. *J. Lipid Res.* **38:** 1963–1972.
54. Clarke, S. D. 2000. Polyunsaturated fatty acid regulation of gene transcription: a mechanism to improve energy balance and insulin resistance. *Br. J. Nutr.* **83 (Suppl. 1):** 59–66.